

Received: 2019.11.04
Accepted: 2020.01.30
Available online: 2020.02.12
Published: 2020.04.04

Anticancer Effect of Radix Astragali on Cholangiocarcinoma *In Vitro* and Its Mechanism via Network Pharmacology

Authors' Contribution:
Study Design A
Data Collection B
Statistical Analysis C
Data Interpretation D
Manuscript Preparation E
Literature Search F
Funds Collection G

ABCDEF 1 **Yixiu Wang***
ABCD 2 **Bingzi Dong***
ADF 1 **Weijie Xue**
BCD 1 **Yujie Feng**
BE 1 **Chenyu Yang**
CF 1 **Peng Liu**
ACFG 1 **Jingyu Cao**
ACFG 1,2 **Chengzhan Zhu**

1 Department of Hepatobiliary and Pancreatic Surgery, Affiliated Hospital of Qingdao University, Qingdao, Shandong, P.R. China
2 Shandong Key Laboratory of Digital Medicine and Computer Assisted Surgery, Affiliated Hospital of Qingdao University, Qingdao, Shandong, P.R. China

* Yixiu Wang and Bingzi Dong contributed equally to this work

Corresponding Authors: Chengzhan Zhu, e-mail: zhuchengzhan@qduhospital.cn, Jingyu Cao, e-mail: c jy7027@163.com
Source of support:

This work was supported by the National Natural Science Foundation of China (No.81600490 and 81600691), the China Postdoctoral Science Foundation (No. 2016M602098 and 2018M640615), the Taishan Scholars Program of Shandong Province (No. 2019010668), and the Qingdao Postdoctoral Science Foundation (No. 2016046)

Background: This study used network pharmacology method and cell model to assess the effects of Radix Astragali (RA) on cholangiocarcinoma (CCA) and to predict core targets and molecular mechanisms.





Material/Methods: We performed an *in vitro* study to assess the effect of RA on CCA using CCK8 assay, the Live-Cell Analysis System, and trypan blue staining. The components and targets of RA were analyzed using the Traditional Chinese Medicine Systems Pharmacology database, and genes associated with CCA were retrieved from the GeneCards and OMIM platforms. Protein-protein interactions were analyzed with the STRING platform. The components-targets-disease network was built by Cytoscape. The TIMER database revealed the expression of core targets with diverse immune infiltration levels. GO and KEGG analyses were performed to identify molecular-biology processes and signaling pathways. The predictions were verified by Western blotting.

Results: Concentration-dependent antitumor activity was confirmed in the cholangiocarcinoma QBC939 cell line treated with RA. RA contained 16 active compounds, with quercetin and kaempferol as the core compounds. The most important biotargets for RA in CCA were caspase 3, MAPK8, MYC, EGFR, and PARP. The TIMER database revealed that the expression of caspase3 and MYC was related with diverse immune infiltration levels of CCA. The results of Western blotting showed RA significantly influenced the expression of the 5 targets that network pharmacology predicted.

Conclusions: RA is an active medicinal material that can be developed into a safe and effective multi-targeted anticancer treatment for CCA.

MeSH Keywords: **Cholangiocarcinoma • Medicine, Chinese Traditional • Pharmacologic Actions**

Full-text PDF: <https://www.medscimonit.com/abstract/index/idArt/921162>

 3177  3  9  74



Background

Cholangiocarcinoma (CCA) is the second most common hepatic malignant tumor, and its incidence has been increasing globally [1,2]. Most patients are in advanced stage. Treatments for patients who have unresectable or advanced CCA are limited. Various chemotherapeutic drugs have been used for treating CCA patients, like 5-fluorouracil, gemcitabine (GEM), cisplatin (CIS), and doxorubicin (DOX) [3], but CCA responds poorly to these drugs [4]. The current median overall survival after standard chemotherapy regimens is less than 1 year [5]. Therefore, it is necessary to develop alternative treatment approaches for CCA.

Humans have used herbs for treating disease for at least 60 000 years [6], showing they have a wide range of pharmacological properties, including anticancer activity [7–9]. Herbal formulae can act on many targets through their various components and play an integral role in key biological processes to exert therapeutic roles during disease development [10]. RA is a traditional Chinese medicine which was listed as being in the top grade in *Shennong' Materia Medica* [11]. Several studies have shown that RA has antitumor activity [12]. RA extracts can inhibit the growth of lung adenocarcinoma cells [13]. Zhang et al. found that concentration-dependent antitumor activity was confirmed in laryngeal carcinoma SCC15 cell line treated with total RA glucosides [14], and RA can effectively promote oral cancer Hep-2 cell line apoptosis [15]. In addition, RA has immune-modulating activities [16]. It was reported that RA can inhibit the phagocytic activity of peritoneal macrophages, promote the transformation of spleen lymphocytes [17], secrete interleukin (IL)-2, and affect the activity of natural killer (NK) cells [17–19]. However, there is no published study that analyzed the effect of RA in treating CCA. Therefore, we performed the present study to assess the effect of RA on CCA and to identify its biological target and molecular mechanism to provide a scientific reference for further research.

Network pharmacology is an emerging and novel approach for exploring the systemic mechanisms of therapeutic compounds in disease [20,21]. The use of network pharmacology to identify herbal targets and potential mechanisms is becoming important to save money, effort, and time needed for drug discovery and design [22,23]. Network pharmacology has successfully realized the construction and visualization of drug–disease–target networks, which is helpful to evaluate the mechanism of drugs from multiple perspectives [24,25]. Network pharmacology can be applied in identifying the pharmacological targets and mechanisms of RA in CCA.

Therefore, we investigated the antitumor activity of RA on CCA in an *in vitro* study. We then used network pharmacology to analysis the core targets and biological functions, pathways,

and mechanisms of RA in treating CCA. We verified the core targets and pathway by Western blotting. A schematic flow-chart of the experiment design is shown in Figure 1.

Material and Methods

Preparation of freeze-dried RA water extract

Radix Astragali (root pieces, origin: Inner Mongolia, China) was purchased from Weifang Hospital of Traditional Chinese Medicine. We prepared aqueous extracts of freeze-dried RA. A total of 15 g of freeze-dried RA pieces was boiled in 500 mL water for 30 min. The water extract solution was concentrated to a volume of 250 mL. Finally, the extract solution was filtrated with a 0.22- μ m filter to remove bacteria and then was maintained at 4°C until use.

Cell lines and cell culture

The CCA cell line QBC939 cells were purchased from the Shanghai Cell Bank of the Chinese Science Academy (Shanghai, China). Cells were cultured in Dulbecco's modified Eagle's medium with 10% fetal bovine serum in a cell culture incubator (Thermo Fisher Scientific, Waltham, MA, USA) at 37°C and 5% CO₂.

Cell viability assay

QBC939 cells (5×10³ cells/well) were plated into 96-well plates and treated with various concentrations of RA (0, 100, 200, and 400 μ g/mL), and PBS was used in the control group. After 24 h, cell viability was assessed by CCK8 assay. We cultured the cells for 1 h with CCK8 agent, then the optical density (OD) was measured at 450 nm on an enzyme-labeling instrument. Additionally, QBC939 cells were seeded into 6-well plates and cultured until the cell density reached 50%. After treatment with various concentrations of RA (0, 100, 200, and 400 μ g/mL), the cells were imaged using an IncuCyte® S3 Live-Cell Analysis System (Essen BioScience) every 1 h, and 9 fields of view were imaged per well.

Trypan blue staining

After being treated with various concentrations of RA (0, 100, 200, and 400 μ g/mL), QBC939 cells were digested and 50- μ L of cell suspension was mixed with 50 μ L trypan blue staining solution. The mixture was placed into a hemacytometer and counted under a microscope within 10 min.

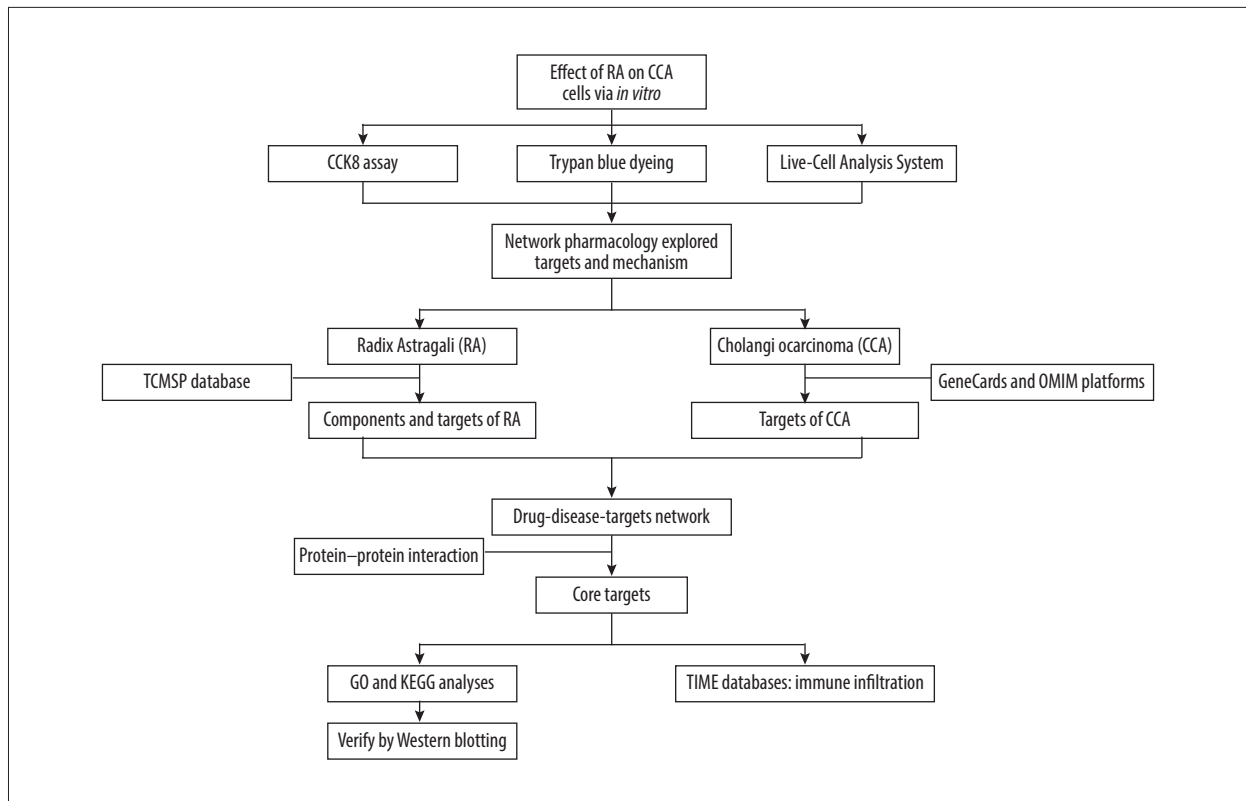


Figure 1. Flowchart of the experimental procedures.

Collection chemical components and targets for RA

To evaluate the pharmacokinetics properties of RA, we used the TCMSP database (<http://lsp.nwu.edu.cn/>) [26] to collect information on chemical components for RA, which is a systems pharmacology resource used to evaluate traditional Chinese medicines or related compounds. With the pharmacokinetic information retrieval filter based on the TCMSP platform, the oral bioavailability (OB) and drug-likeness (DL) were set to $\geq 30\%$ and ≥ 0.18 to obtain qualified herbal compounds. The chemical structures of the compounds were drawn using ChemBioOffice 2010.

Collection of disease targets

Potential genes associated with CCA were collected from GeneCards (<https://www.genecards.org/>) [27] with the keyword “cholangiocarcinoma” and Online Mendelian Inheritance in Man (OMIM) (<https://www.omim.org/>) [28] with the keyword “bile duct carcinoma”.

Construction of components–targets–disease network

Venny2.1.0 (<http://bioinfogp.cnb.csic.es/tools/venny/>) [29] was used to screen for common RA targets and CCA-related targets. Cytoscape-v3.7.1 [30] software was used to create the

model of the target–disease and component–target network, and the Merge function was used to construct the component–target–disease network model. Results were further analyzed to determine the mutual relationships in the network model.

Protein–protein interaction (PPI) data

The Search Tool for the Retrieval of Interacting Genes (STRING) database (<https://string-db.org/>, ver.10.5) [31] was used to analyze protein–protein interactions of the common targets from the RA targets and CCA-related targets. The database defines PPIs with confidence ranges for data scores; in the present study, PPIs with medium confidence (0.4) were further examined.

Gene function and pathway enrichment analysis

clusterProfiler [32] is an R package for comparing biological themes among gene clusters, which can be used to analyze functional and pathway enrichment information on the gene of interest. The common targets were input into the R 3.6.0 platform by clusterProfiler software, using an enrichment analysis method with the Gene Ontology (GO) [33] and Kyoto Encyclopedia of Genes and Genomes (KEGG) [34] databases. Enriched GO terms were defined and relevant pathways with p values < 0.05 were selected. Target–pathway and

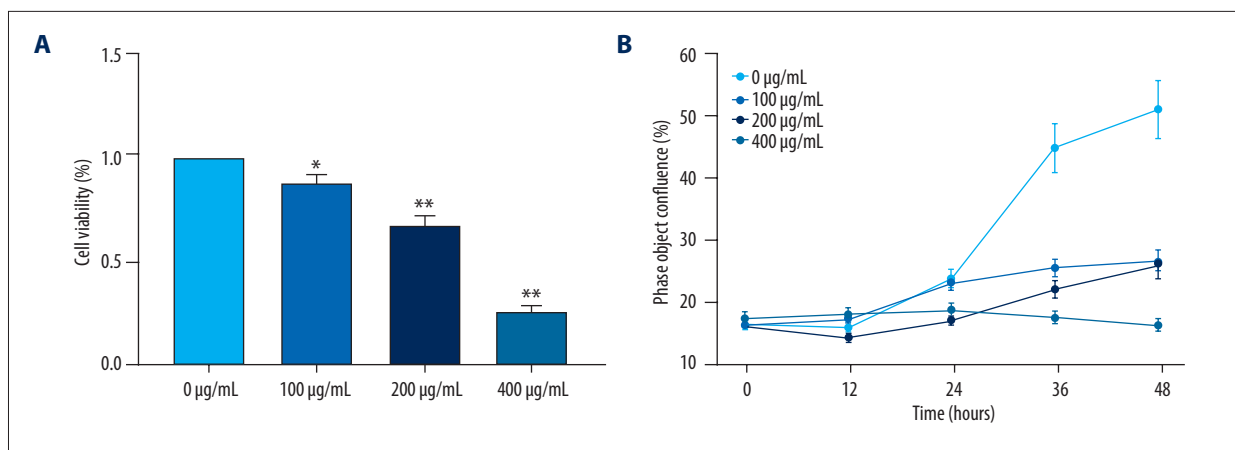


Figure 2. RA inhibits CCA cell proliferation: (A) RA inhibited the viability of QBC939 cells in a dose-dependent manner with CCK8 assay; (B) The numbers of QBC939 cells increased slowly after RA treatment. Values represent means \pm SD, n=5, * $P<0.05$, ** $P<0.01$ compared with 0 $\mu\text{g/mL}$ group.

constituent–pathway networks were built to show an overview of the interactions between RA targets and CCA [35].

Analysis of gene expression and tumor-infiltrating immune cells

Using the online tool TIMER (<https://cistrome.shinyapps.io/timer/>) [36], we investigated the correlation between the expression of core targets and tumor-infiltrating immune cells (B cells, CD4+ T cells, CD8+ T cells, neutrophils, macrophages, and dendritic cells) in CCA, which is a comprehensive resource for systematic analysis of immune infiltrates across diverse cancer types [37].

Western blotting analysis

Total protein was extracted from QBC939 cells after RA treatment (0, 100, 200, and 400 $\mu\text{g/mL}$) and separated by sodium dodecyl sulfate-polyacrylamide gel electrophoresis, followed by transfer of the proteins onto a polyvinylidene fluoride membrane (Millipore, Billerica, MA, USA). The primary antibodies were: caspase3 (NO.9662; Cell Signaling Technology, Danvers, MA, USA), SAPK/JNK (NO.9252; Cell Signaling Technology), p-SAPK/JNK (NO.4668; Cell Signaling Technology), c-MYC (NO.9402; Cell Signaling Technology), EGFR (NO.4267; Cell Signaling Technology), p-EGFR (NO.3777; Cell Signaling Technology), and PARP (NO.9542; Cell Signaling Technology).

Statistical analysis

Statistical analysis was performed using the SPSS program (version 23.0). All the data are presented as means \pm standard deviation. Differences were evaluated by Student's *t* test, with $p<0.05$ considered statistically significant.

Results

RA inhibits the cell proliferation of QBC939 cells

After incubating the cells with various concentrations of RA (0, 100, 200, and 400 $\mu\text{g/mL}$) for 24 h, it was found that all tested concentrations of RA inhibited the proliferation of QBC939 cells with the CCK8 assay ($p<0.05$). Compared with the control group, growth inhibition increased in a concentration-dependent manner (100, 200, 400 $\mu\text{g/mL}$) (Figure 2A). The IncuCyte® S3 Live-Cell Analysis System was used to image surviving cells, which clearly revealed the gradual decrease in the numbers of QBC939 cells with increasing concentration (Figure 2B). RA also influenced the morphological characteristics and adherence of the cells to the plate; the cells displayed apoptotic morphology (Supplementary Figure 1).

Trypan blue counting analysis

Trypan blue staining is often applied to detect cell death. As shown in Figure 3, the living cells are non-stained, while dead cells are dyed blue. After counting the dead cells and living cells, we calculated the cell viability. The results showed that compared with the control group, the cell viability significantly decreased in a concentration-dependent manner after treatment with RA ($p<0.05$).

Screening results of components and target proteins

Using the TCMSP database, 20 herbal compounds were identified, 16 of which had corresponding targets. The 97 targets of the 16 compounds were obtained and the details are presented in Table 1. These 97 identified targets were further investigated.

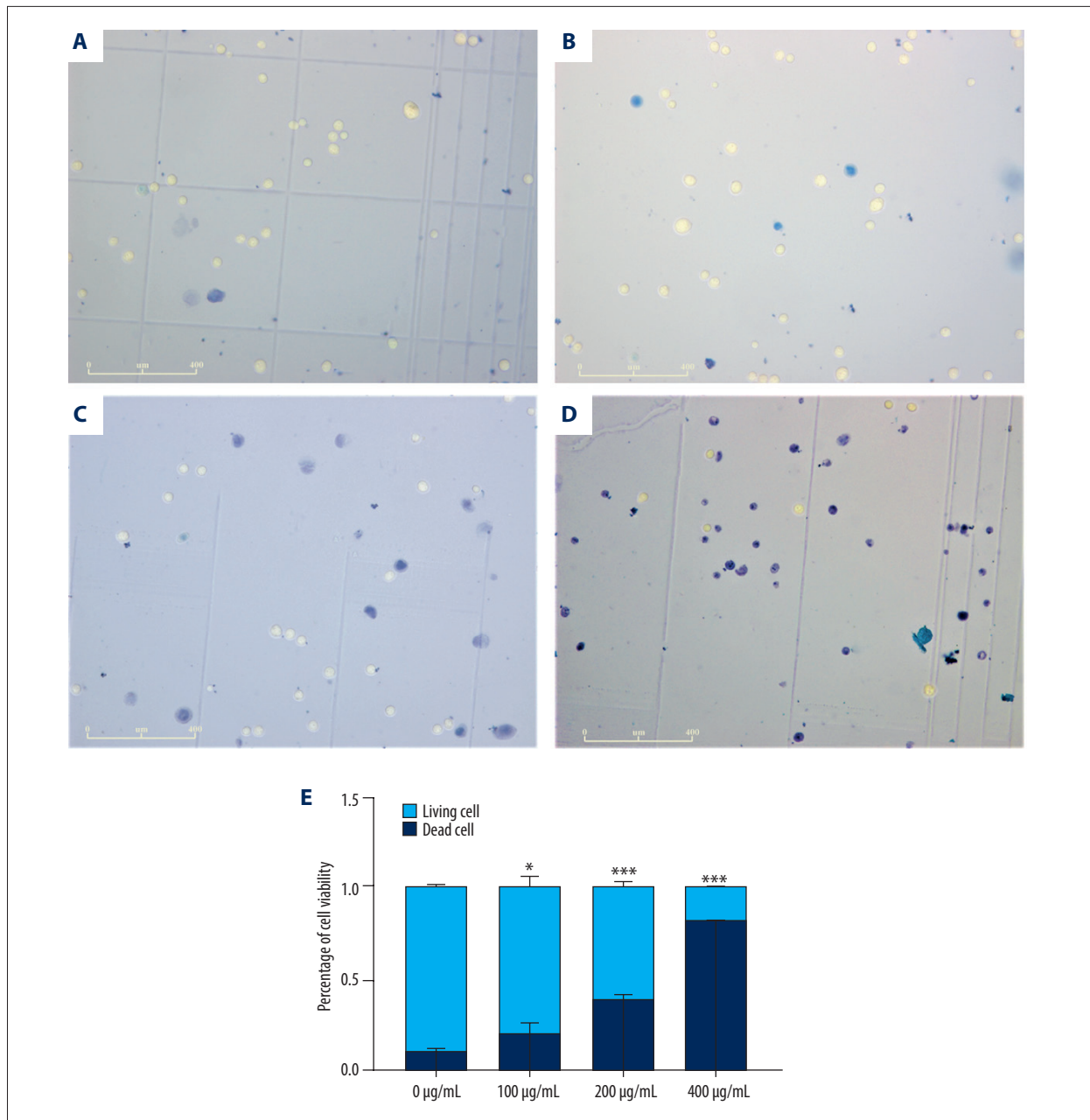


Figure 3. The effect of RA on QBC939 cells detected by trypan blue staining assay. (A–D) Represents 0, 100, 200, 400 µg/mL, respectively. (E) Shows histogram analysis. Values represent means±SD, n=3, * $P<0.05$, ** $P<0.01$, *** $P<0.001$ compared with 0 µg/mL group.

Results of CCA targets

We acquired 1452 known correlated targets from GeneCards, and 83 known related targets were acquired from OMIM. After redundant names were deleted, 1529 known CCA-related targets were collected, and the list of targeted genes is shown in Supplementary Table 1.

Network construction

Of the 1529 known cholangiocarcinoma-related targets, 50 targets are involved in RA, and through Venny 2.1.0, the common targets were obtained, including PGR, PTGS1, CHEK1, PRSS1, CHRM3, ESR1, PPARG, GSK3B, F7, BCL2, CASP3, MAPK8, CYP1A1, SELE, ALOX5, GSTP1, AHR, NR1I3, GSTM1, EGFR, VEGFA, CCND1, CASP9, PLAU, RB1, IL6, TP63, ELK1, CASP8, RAF1, PRKCA, HIF1A, ERBB2, MYC, PTGER3, BIRC5, NOS3, HSPB1, CCNB1, NFE2L2,

Table 1. Potential active compounds in HMM.

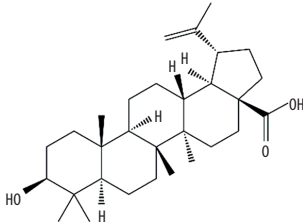
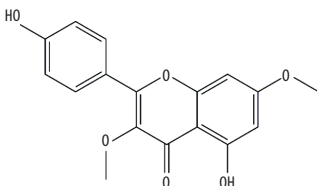
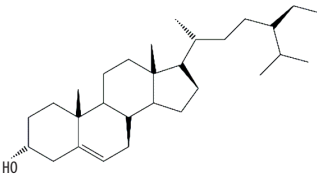
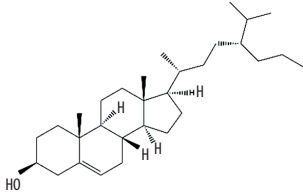
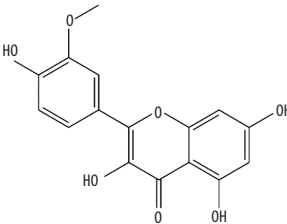
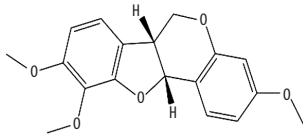
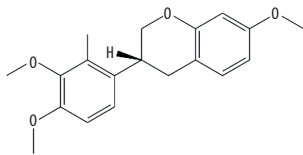
Molecule ID	Molecule name	OB (%)	DL	Chemical structure
MOL000211	Mairin	55.38	0.78	
MOL000239	Jaranol	50.83	0.29	
MOL000296	Hederagenin	36.91	0.75	
MOL000033	(3S,8S,9S,10R,13R,14S,17R)-10,13-dimethyl-17-[(2R,5S)-5-propan-2-yl-octan-2-yl]-2,3,4,7,8,9,11,12,14,15,16,17-dodecahydro-1H-cyclopenta[a]phenanthren-3-ol	36.23	0.78	
MOL000354	Isorhamnetin	49.6	0.31	
MOL000371	3,9-di-O-methylnissolin	53.74	0.48	
MOL000378	7-O-methylisomucronulatol	74.69	0.3	

Table 1 continued. Potential active compounds in HMM.

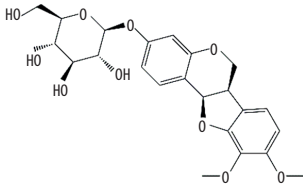
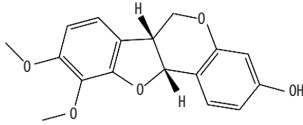
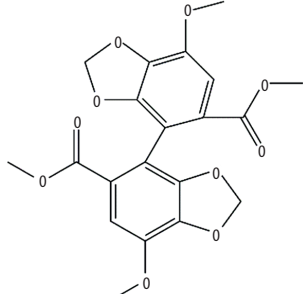
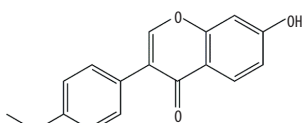
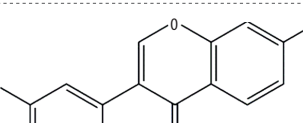
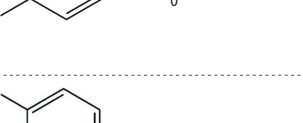
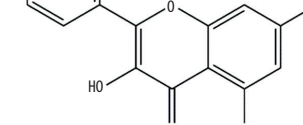
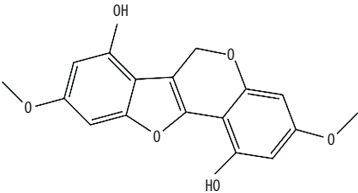
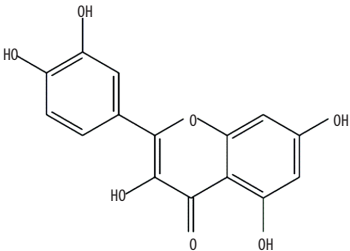
Molecule ID	Molecule name	OB (%)	DL	Chemical structure
MOL000379	9,10-dimethoxypterocarpan-3-O-β-D-glucoside	36.74	0.92	
MOL000380	(6aR,11aR)-9,10-dimethoxy-6a,11a-dihydro-6H-benzofurano[3,2-c]chromen-3-ol	64.26	0.42	
MOL000387	Bifendate	31.1	0.67	
MOL000392	Formononetin	69.67	0.21	
MOL000417	Calycosin	47.75	0.24	
MOL000422	Kaempferol	41.88	0.24	
MOL000433	FA	68.96	0.71	

Table 1 continued. Potential active compounds in HMM.

Molecule ID	Molecule name	OB (%)	DL	Chemical structure
MOL000442	1,7-Dihydroxy-3,9-dimethoxy pterocarpene	39.05	0.48	
MOL000098	Quercetin	46.43	0.28	

NQO1, PARP1, CHEK2, HSF1, CRP, RASSF1, IRF1, ERBB3, PON1, and HK2, which all act on the pathway of treating cholangiocarcinoma by RA (Figure 4A, Table 2).

The 50 green nodes represent the target of cholangiocarcinoma, and the 15 pink nodes represent the target protein of the RA compounds. Network construction of compound disease targets consists of 67 nodes and 172 edges. Among them, 65 nodes and 107 edges directly reflect the interaction between the RA targets and cholangiocarcinoma targets (Figure 4B).

PPI network of common targets

Protein–protein interactions (PPI) of the 50 disease-related targets were analyzed using the PPI network. After setting the interaction score to medium confidence and hiding disconnected nodes in the network, the PPI network contained 48 nodes and 361 edges (Figure 5A), with a 14.4 average node degree and PPI enrichment p value $<1.0e-16$, showing the multi-target characteristics of RA. According to the degree of nodes exported from the STRING database, the order of key targets was analyzed, and the top 30 nodes with a degree ≥ 10 were selected (Figure 5B).

GO and KEGG pathway analysis

GO and KEGG analyses were performed to further study the biological process of the 50 common targets. As shown in Figure 6A, the top 10 significantly enriched GO terms (adjusted p value <0.001) were used and included the response to ubiquitin-like protein ligase binding, DNA-binding transcription activator activity, RNA polymerase II-specific, nuclear receptor activity, transcription factor activity, direct ligand regulated

sequence-specific DNA binding, proximal promoter sequence-specific DNA binding, ubiquitin protein ligase binding, protein heterodimerization activity, RNA polymerase II proximal promoter sequence-specific DNA binding, Hsp90 protein binding, and E-box binding. The results were highly correlated with anticancer activities, demonstrating that RA exerted its effects against CCA by engaging in the above biological processes and cell functions.

Furthermore, these 50 genes participated in 79 KEGG pathways with adjusted p values <0.01 ; after sorting the adjusted p values, the top 20 were analyzed (Figure 6B).

Association of core targets' expression with CCA purity and immune infiltration

The tumor microenvironment includes cancer cells, matrix cells, and infiltrating immune cells. Infiltrating immune cells are an independent predictor of sentinel lymph node status and survival of cancer patients [38,39]. Tumor purity plays a role in analyzing immune infiltration in clinical tumor samples by genomics methods [40]. The expressions of caspase3 and MYC were significantly negatively correlated with tumor purity via TIMER platform, while EGFR and PARP were not associated with tumor purity. Interestingly, we found expression of caspase3 was positively correlated with infiltration level of B cells in CCA, and expression of MYC was positively correlated with the infiltration level of B cells, CD4+ cells, macrophages, neutrophils, and dendritic cells in CCA (Figure 7A, 7B).

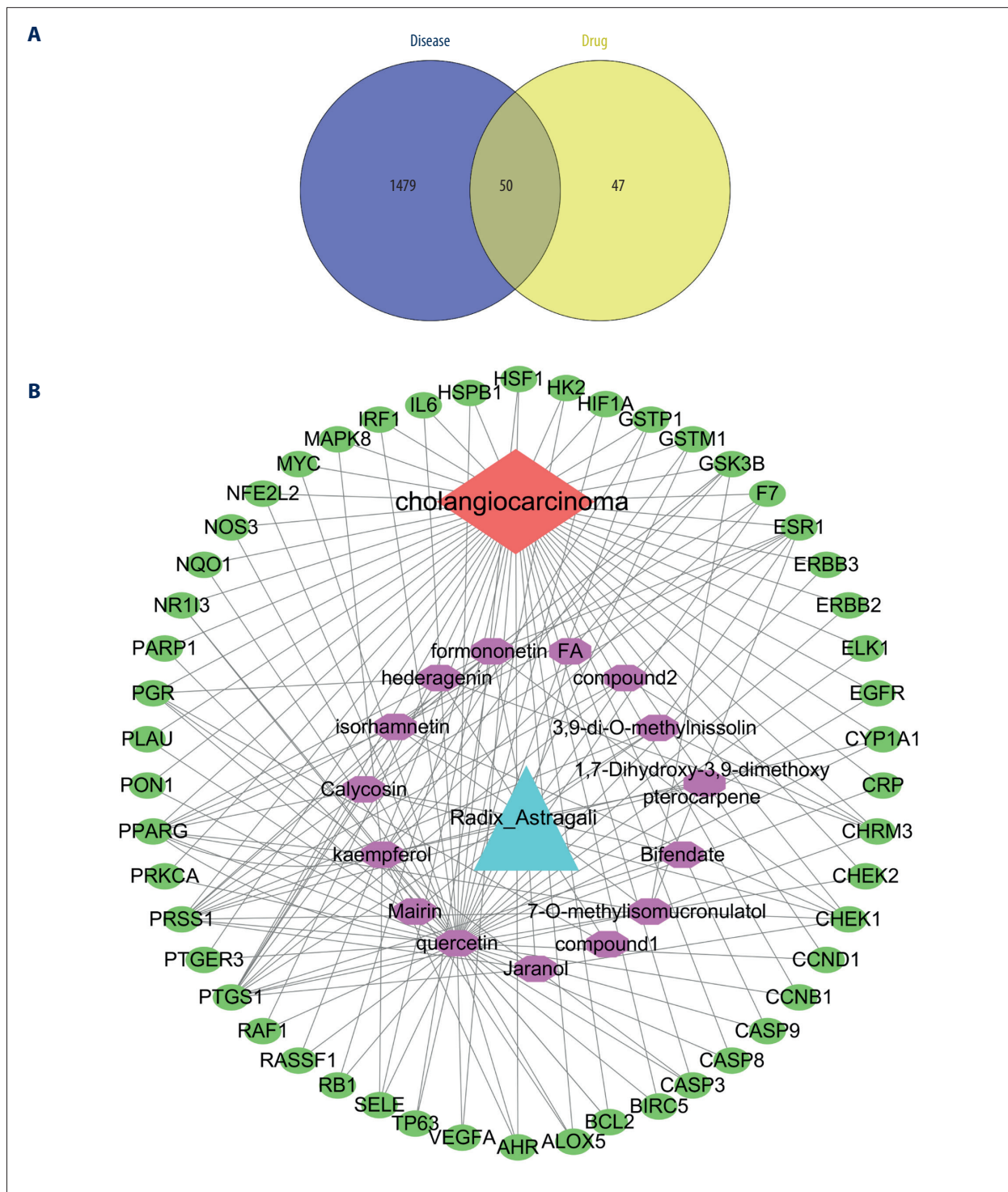


Figure 4. Network construction of compound disease targets. **(A)** Venn diagram shows common part between RA with cholangiocarcinoma (CCA). **(B)** Network of RA compound targets and CCA targets. Note: drug compound1 represents (3S,8S,9S,10R,13R,14S,17R)-10,13-dimethyl-17-[(2R,5S)-5-propan-2-yl-octan-2-yl]-2,3,4,7,8,9,11,12,14,15,16,17-dodecahydro-1H-cyclopenta[a]phenanthren-3-ol; compound2 represents (6aR,11aR)-9,10-dimethoxy-6a,11a-dihydro-6H-benzofurano[3,2-c]chromen-3-ol.

Table 2. Common targets between HMM and cholangiocarcinoma.

Gene ID	Gene symbol	Gene name
5241	PGR	Progesterone receptor
5742	PTGS1	Prostaglandin G/H synthase 1
1111	CHEK1	Serine/threonine-protein kinase Chk1
5644	PRSS1	Trypsin-1
1131	CHRM3	Muscarinic acetylcholine receptor M3
2099	ESR1	Estrogen receptor
5468	PPARG	Peroxisome proliferator activated receptor gamma
2932	GSK3B	Glycogen synthase kinase-3 beta
2155	F7	Coagulation factor VII
596	BCL2	Apoptosis regulator Bcl-2
836	CASP3	Caspase-3
5599	MAPK8	Mitogen-activated protein kinase 8
1543	CYP1A1	Cytochrome P450 1A1
6401	SELE	E-selectin
240	ALOX5	Arachidonate 5-lipoxygenase
2950	GSTP1	Glutathione S-transferase P
196	AHR	Aryl hydrocarbon receptor
9970	NR1B3	Nuclear receptor subfamily 1 group I member 3
2944	GSTM1	Glutathione S-transferase Mu 1
1956	EGFR	Epidermal growth factor receptor
7422	VEGFA	Vascular endothelial growth factor A
595	CCND1	G1/S-specific cyclin-D1
842	CASP9	Caspase-9
5328	PLAU	Urokinase-type plasminogen activator
5925	RB1	Retinoblastoma-associated protein
3569	IL6	Interleukin-6
8626	TP63	Cellular tumor antigen p53
2002	ELK1	ETS domain-containing protein Elk-1
841	CASP8	Caspase-8
5894	RAF1	RAF proto-oncogene serine/threonine-protein kinase
5578	PRKCA	Protein kinase C alpha type
3091	HIF1A	Hypoxia-inducible factor 1-alpha
2064	ERBB2	Receptor tyrosine-protein kinase erbB-2
4609	MYC	MYC proto-oncogene protein
5733	PTGER3	Prostaglandin E2 receptor EP3 subtype

Table 2 continued. Common targets between HMM and cholangiocarcinoma.

Gene ID	Gene symbol	Gene name
332	BIRC5	Baculoviral IAP repeat-containing protein 5
4846	NOS3	Nitric oxide synthase, endothelial
3315	HSPB1	Heat shock protein beta-1
891	CCNB1	G2/mitotic-specific cyclin-B1
4780	NFE2L2	Nuclear factor erythroid 2-related factor 2
1728	NQO1	NAD(P)H dehydrogenase [quinone] 1
142	PARP1	Poly [ADP-ribose] polymerase 1
11200	CHEK2	Serine/threonine-protein kinase Chk2
3297	HSF1	Heat shock factor protein 1
1401	CRP	C-reactive protein
11186	RASSF1	Ras association domain-containing protein 1
3659	IRF1	Interferon regulatory factor 1
2065	ERBB3	Receptor tyrosine-protein kinase erbB-3
5444	PON1	Serum paraoxonase/arylesterase 1
3099	HK2	Hexokinase-2

Changes in core target expression

To verify the core targets in the network of RA and CCA, we investigated the expression of core target proteins by Western blotting in QBC939 cells treated with RA, and found that RA downregulated the P-EGFR/EGFR and p-MAPK8/MAPK8 ratios, upregulated the cleaved caspase3/caspase3 ratio, and reduced the expression of c-MYC and PARP (Figure 8A, 8B). Western blotting results showed concentration-dependent antitumor activity in QBC939 cells treated with RA through these targets ($p < 0.05$).

Discussion

Cholangiocarcinoma is a relatively common malignant tumor derived from the intrahepatic. Due to difficulties in detection and drug resistance, it is very important to explore the regulation of CCA biological characteristics and find new treatment methods for multi-modal management of CCA.

Network pharmacology can improve drug efficacy and the success rate of clinical trials, as well as decrease in the costs of drug discovery via exploring the regulation of signaling pathways with multiple channels [42]. In our study, the network pharmacology findings from web-based databases revealed core gene targets, and we explored the biological functions,

pathways, and mechanisms of RA in CCA. These findings support that RA is a promising resource with specific therapeutic effects on CCA.

RA is a type of astragalus, and several studies have shown that astragalus is associated with antitumor [12] and immunomodulating activities [16]. In network pharmacology analysis, the network of compound disease targets revealed quercetin and kaempferol as key active ingredients in RA responsible for the therapeutic effects against CCA. Several studies have suggested that quercetin is helpful for treating CCA as a dietary phytochemical with anti-inflammatory and antitumor effects [43,44] and may be useful against CCA as a cancer chemopreventive drug. Kaempferol has antioxidant, anti-inflammatory, and antitumor activities [45–47]. Qin et al. [48] showed that kaempferol has potent effects against CCA both *in vitro* and *in vivo* via the PI3K/AKT pathway, which is involved in apoptosis, proliferation, and invasion. In our *in vitro* study, the RA extract was cytotoxic and inhibited the proliferation of the bile duct carcinoma cell line QBC939.

Important predictive biotargets for RA in CCA were identified as caspase3, MAPK8, MYC, EGFR, and PARP. Caspase3, a cysteine-aspartic acid protease, plays a central role in the execution phase of cell apoptosis. As an executioner caspase, the caspase3 zymogen has activity after it is cleaved by an initiator caspase when apoptotic signaling events have occurred [49].

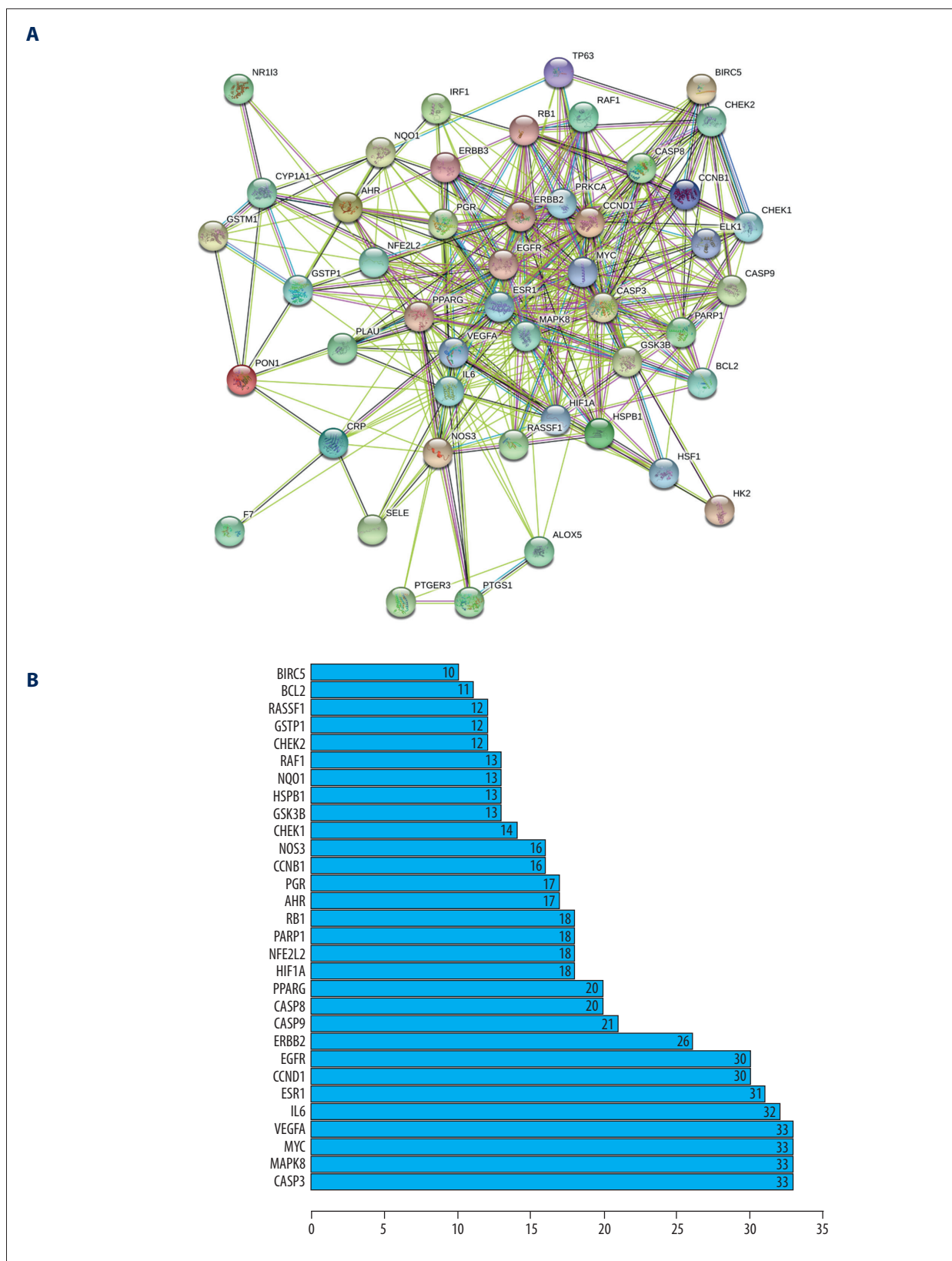


Figure 5. PPI network of common targets. (A) Nodes mean targets and colors of edges means different relationships. (B) Top 30 nodes are likely key proteins in the interaction of cholangiocarcinoma.

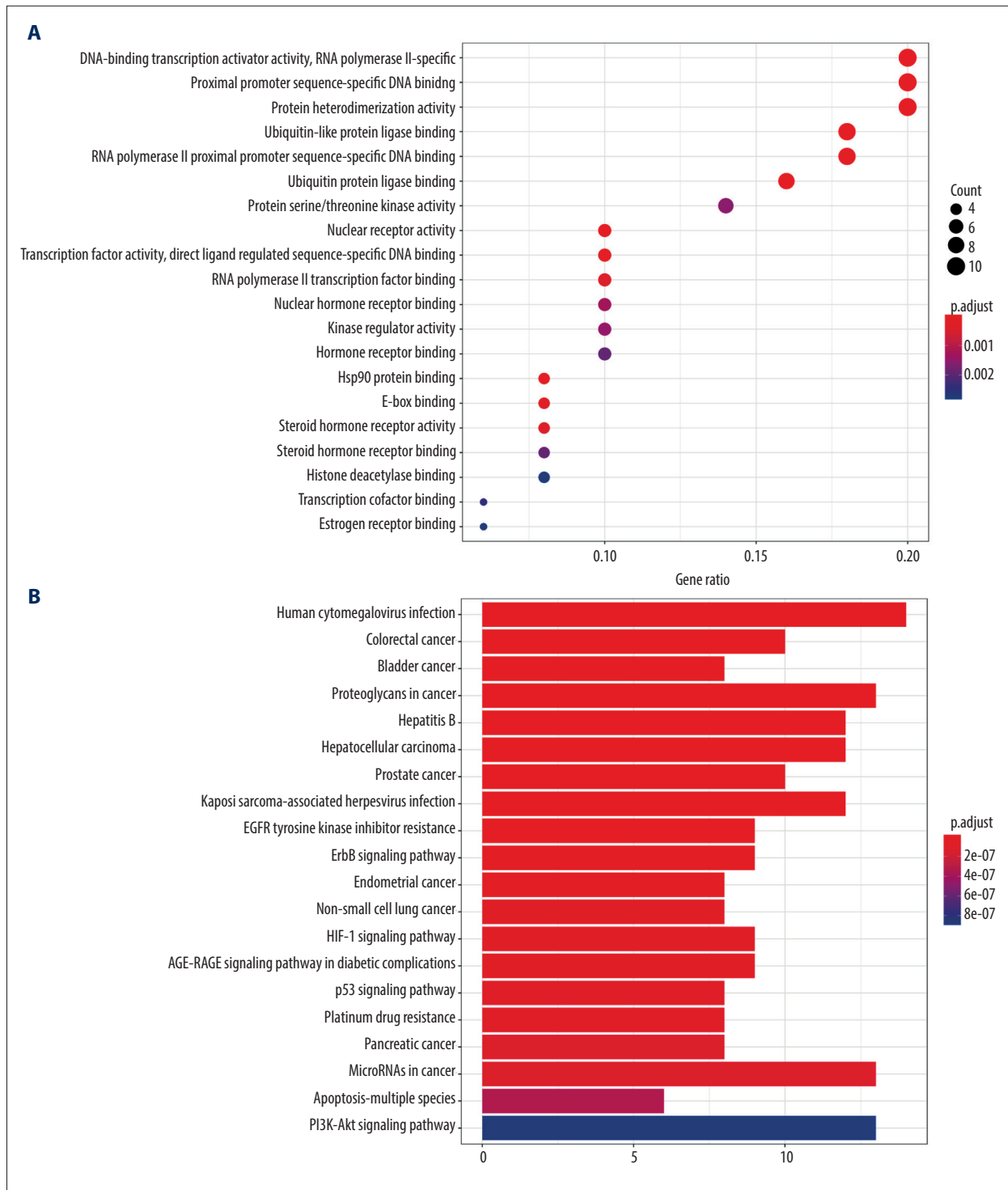


Figure 6. GO and pathway analysis. **(A)** GO analysis of common targets of RA and cholangiocarcinoma. The Y-axis represents significant GO biological function processes and the X-axis represents the counts of enriched targets. The gradient of color represents the different adjusted p values. **(B)** KEGG analysis for common targets of RA and cholangiocarcinoma. The Y-axis represents significant KEGG pathways and the X-axis represents the ratio of enriched targets in a pathway to all common targets. The size of the nodes shows count of targets, and gradient of color represents the adjusted p value.

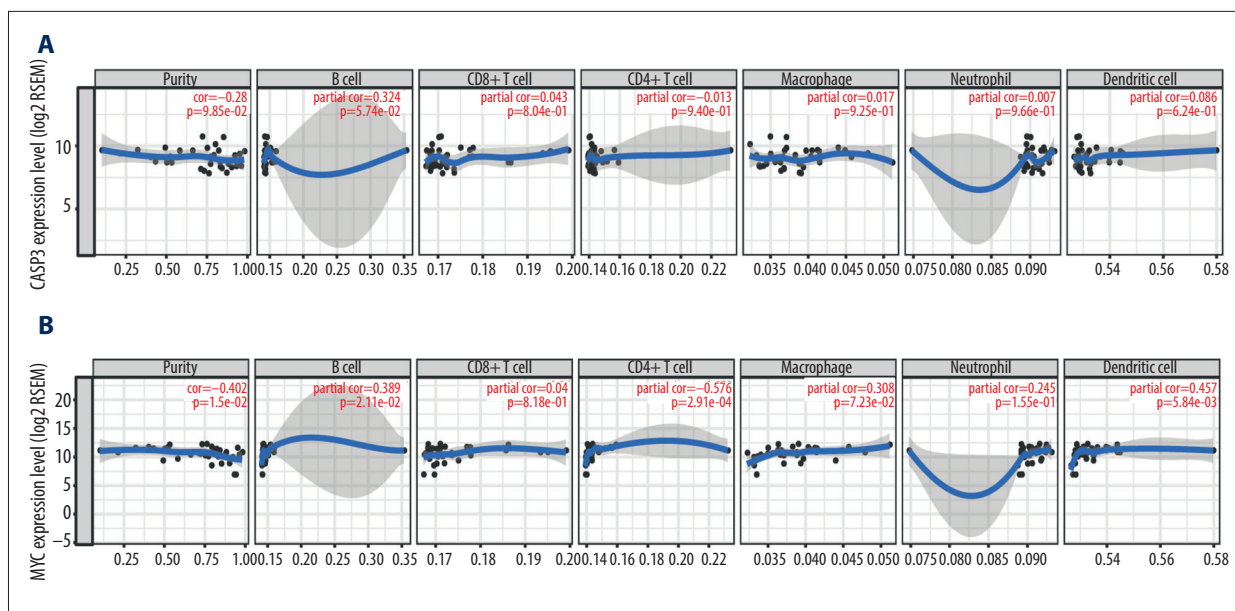


Figure 7. Correlation of core target expression with immune infiltration level in CCA. **(A)** Caspase3 expression level is significantly negatively related to tumor purity and positively related to the infiltration level of B cells in CCA. **(B)** MYC expression level is significantly negatively related to tumor purity and positively related to the infiltration level of B cells, CD4+ cells, macrophages, neutrophils, and dendritic cells in CCA.

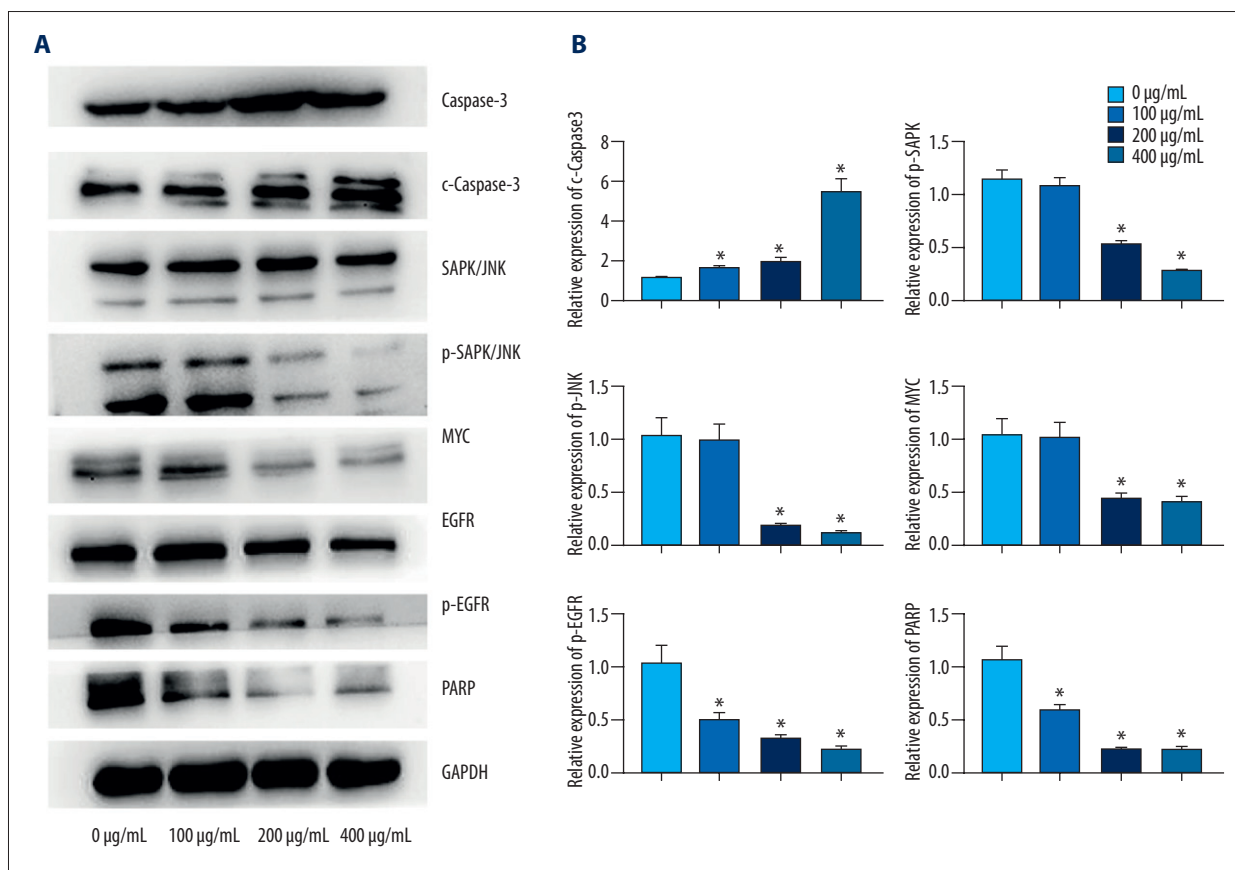


Figure 8. **(A, B)** Changes in core target proteins in QBC939 cells after RA treatment. GAPDH was used as loading control. n=3, * p<0.05 compared with 0 µg/mL group.

Caspase3 plays a dominant role in the hallmark caspase cascade, which is characteristic of the apoptotic pathway triggered by extrinsic activation [50]. MAPK8, a transduction protein, controls several cellular processes, including cell proliferation and survival [51]. Nishikawa et al. reported that MAPK signaling appears to induce a biliary proliferation program in hepatocytes or liver bipotential cells, implicating this pathway in human CCA [52]. In human intrahepatic CCA, TNF is highly expressed near intrahepatic CCA lesions, and CCA p-JNK, and reactive oxygen species (ROS) accumulation in surrounding hepatocytes are present, causing cholangiocellular proliferation/differentiation and carcinogenesis. Targeting the ROS/TNF/JNK axis may improve intrahepatic CCA therapy [53].

C-MYC is the most well-known and studied member of the MYC oncoprotein family and it is estimated that in up to 70% of human cancers, c-MYC expression is elevated or deregulated through different mechanisms and is associated with an invasive cancer phenotype [54]. Many studies have demonstrated that c-MYC induction promotes cholestatic liver injury and CCA progression [55]. EGFR belongs to the HER/ErbB family of tyrosine kinase receptors. In many types of cancer, EGFR activation inhibits cell–cell adhesion by destabilizing the complex of E-cadherin/ β -catenin, promotes tumor metastasis, and contributes to the procurement of a motile phenotype [56–58]. In CCA, overexpression of EGFR is related to tumor progression [59–64], and the EGF/EGFR axis contributes to epithelial-mesenchymal transition in CCA tumor cells, promoting the progression of this type of cancer [65]. PARP is a nuclear DNA-binding protein and is an important component involved in single-strand break damage repair [66]. Upon DNA damage, PARP-1 catalyzes the PARylation of acceptor proteins and repairs damaged DNA via base excision repair to maintain genomic stability [67]. PARP inhibitors can theoretically enhance tumor cell death, and combining PARP inhibitors such as olaparib with radiation may contribute to treatment of CCA [68].

To further explore the biological functions of the core targets, we used to TIMER database. The expression of caspase3 and MYC was negatively associated with tumor purity, which is correlated with diverse immune infiltration levels in CCA. Caspase3 expression levels are positively associated with the infiltration level of B cells in CCA, and the MYC expression level is positively associated with the infiltration level of B cells, CD4+ cells, macrophages, neutrophils, and dendritic cells in CCA. The results of TIMER suggest that the functions of core targets are related to immunological regulation of the tumor

microenvironment. Immune infiltration is an emerging hallmark of cancer and plays an important role in tumor initiation and progression [69,70]. The tumor microenvironment is a key determinant in distant metastasis and development, in which evolution of the tumor can be traced back to immune-escaping clones [71]. Based on the relationship between the core genes and immune infiltration, RA may inhibit tumor initiation and progression by regulating the tumor microenvironment.

The KEGG results showed that RA regulates the EGFR tyrosine kinase inhibitor resistance pathway as the pharmacological mechanisms of the therapeutic effect of RA against CCA. An EGFR inhibitor was the first targeted drug used for tumor therapy and has been approved for treating metastatic non-small-cell lung cancer, pancreatic cancer, colorectal cancer, and squamous cell carcinoma of the head and neck [72]. As EGFR expression is decreased, downstream signaling in malignant tumor cells is inhibited, leading to inhibition of metastasis, growth, proliferation, differentiation, and angiogenesis and increased cancer cell apoptosis [73]. However, nearly all tumors acquire EGFR tyrosine kinase inhibitor resistance after various periods of time [74].

In our study, the Western blotting results showed that RA downregulated the P-EGFR/EGFR and p-MAPK8/MAPK8 ratios, upregulated the cleaved caspase3/caspase3 ratio, and reduced the expression of c-MYC and PARP. These *in vitro* results support the network pharmacology data and demonstrate that RA affects protein expression of core genes and alters the EGFR tyrosine kinase inhibitor resistance pathway. RA inhibits CCA progression by promoting cell apoptosis and blocking cell proliferation/differentiation and carcinogenesis.

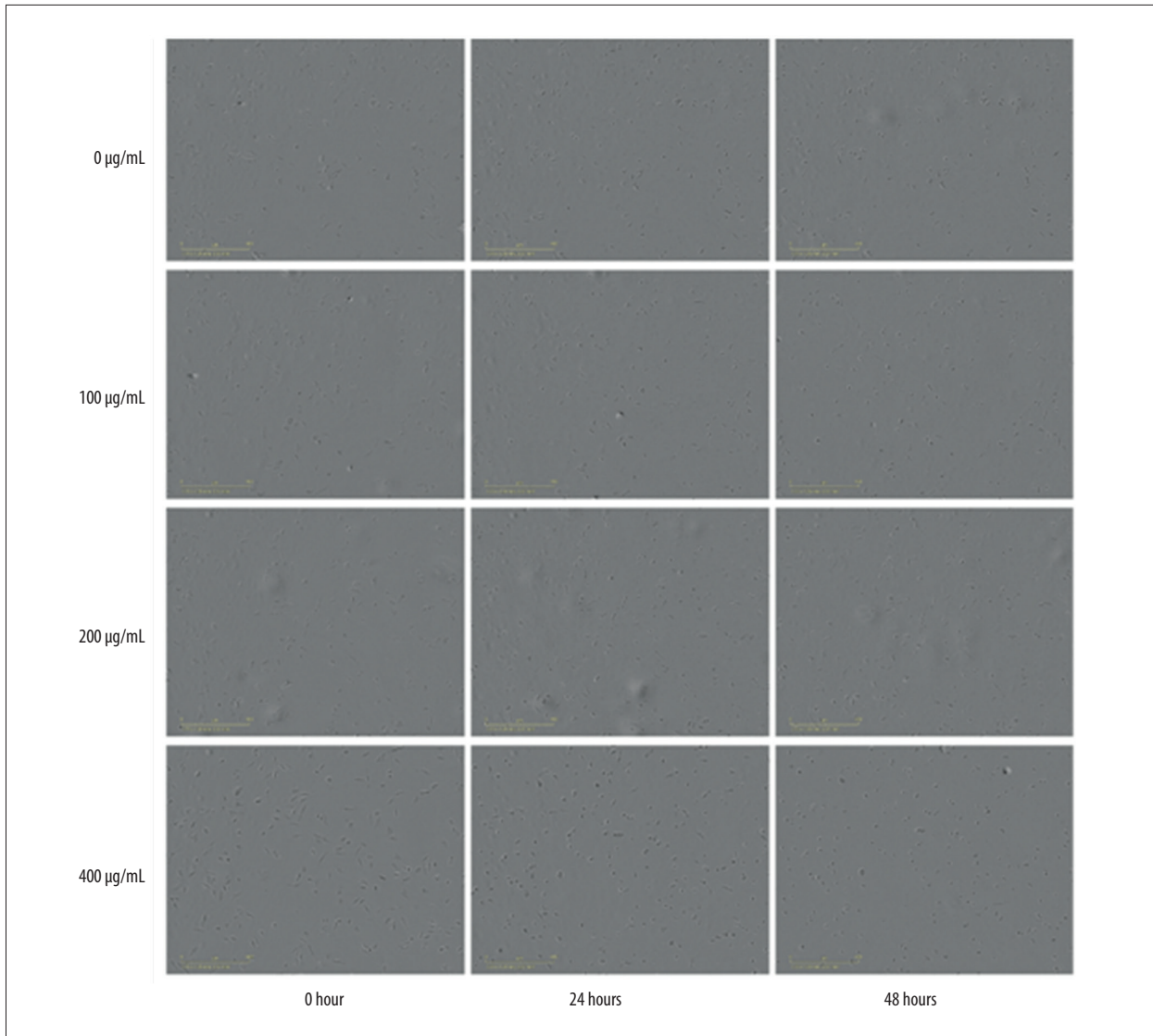
Conclusions

RA appears to be an effective drug when used as adjuvant therapy. The core targets identified included caspase3, MAPK8, MYC, EGFR, and PARP in the network of RA and CCA, indicating potential as therapeutic biomolecules for treating CCA. Further studies are needed to demonstrate that RA is an active plant medicinal material useful for developing a safe and effective multi-targeted anticancer treatment for CCA.

Conflict of interests

None.

Supplementary Data



Supplementary Figure 1. The cells were imaged using the IncuCyte® S3 Live-Cell Analysis System. RA influenced the morphological characteristics and adherence of the cells to the plate.

Supplementary Table 1. Targets from OMIM.

Gene/locus	Gene/locus name	Gene/locus MIM number
BCC1	Basal cell carcinoma, susceptibility to, 1	605462
MYCL	Oncogene MYC, lung carcinoma-derived	164850
LMYC	Oncogene MYC, lung carcinoma-derived	164850
BCAS2	Breast carcinoma amplified sequence 2	605783
DAM1	Breast carcinoma amplified sequence 2	605783
PRN1	Papillary thyroid carcinoma with papillary renal neoplasia	605642
PTCPRN	Papillary thyroid carcinoma with papillary renal neoplasia	605642
RCCP1	Papillary renal cell carcinoma, translocation-associated	179755
PRCC	Papillary renal cell carcinoma, translocation-associated	179755
BCC2	Basal cell carcinoma, susceptibility to, 2	613058
NMTC3	Nonmedullary thyroid carcinoma 3	606240
ABCB11	ATP-binding cassette, subfamily B, member 11 (bile salt export pump)	603201
BSEP	ATP-binding cassette, subfamily B, member 11 (bile salt export pump)	603201
SPGP	ATP-binding cassette, subfamily B, member 11 (bile salt export pump)	603201
PFIC2	ATP-binding cassette, subfamily B, member 11 (bile salt export pump)	603201
BRIC2	ATP-binding cassette, subfamily B, member 11 (bile salt export pump)	603201
BG37	G protein-coupled bile acid receptor 1	610147
GPBAR1	G protein-coupled bile acid receptor 1	610147
FAM107A	Family with sequence similarity 107, member A (downregulated in renal cell carcinoma 1)	608295
TU3A	Family with sequence similarity 107, member A (downregulated in renal cell carcinoma 1)	608295
FAM107A	Family with sequence similarity 107, member A (downregulated in renal cell carcinoma 1)	608295
DIRC2	Disrupted in renal carcinoma 2	602773
RCC4	Disrupted in renal carcinoma 2	602773
MNDEC	Microtia with nasolacrimal duct imperforation and eye coloboma	611863
NPC1	Nasopharyngeal carcinoma 1	607107
NPCA1	Nasopharyngeal carcinoma 1	607107
LOC344967	Acyl-CoA thioesterase 7-like	611963
SOAT	Solute carrier family 10 (sodium/bile acid cotransporter family), member 6	613366
SLC10A6	Solute carrier family 10 (sodium/bile acid cotransporter family), member 6	613366
SLC10A7	Solute carrier family 10 (sodium/bile acid cotransporter family), member 7	611459
SSASKS	Solute carrier family 10 (sodium/bile acid cotransporter family), member 7	611459
BCC3	Basal cell carcinoma, susceptibility to, 3	613059
NPCA2	Nasopharyngeal carcinoma, susceptibility to, 2	161550
BCC6	Basal cell carcinoma, susceptibility to, 6	613063
AKR1D1	Bile acid synthesis defect, congenital, 2	604741
SRD5B1	Bile acid synthesis defect, congenital, 2	604741

Gene/locus	Gene/locus name	Gene/locus MIM number
CBAS2	Bile acid synthesis defect, congenital, 2	604741
NCRNA00197	Papillary thyroid carcinoma susceptibility candidate 1 gene	617440
PTCSC1	Papillary thyroid carcinoma susceptibility candidate 1 gene	617440
BCC5	Basal cell carcinoma, susceptibility to, 5	613062
BAAT	Bile acid coenzyme A: amino acid N-acyltransferase (glycine N-choloyltransferase)	602938
CEL	Carboxyl-ester lipase (bile-salt stimulated lipase)	114840
BSSL	Carboxyl-ester lipase (bile-salt stimulated lipase)	114840
CELL	Carboxyl-ester lipase (bile-salt stimulated lipase)	114840
MODY8	Carboxyl-ester lipase (bile-salt stimulated lipase)	114840
SART1	Squamous cell carcinoma antigen recognized by T cells 1	605941
HOMS1	Squamous cell carcinoma antigen recognized by T cells 1	605941
ANC	Anal canal carcinoma	105580
BCC4	Basal cell carcinoma, susceptibility to, 4	613061
AQP2	Aquaporin-2 (collecting duct)	107777
SART3	Squamous cell carcinoma antigen recognized by T cells 3	611684
P100	Squamous cell carcinoma antigen recognized by T cells 3	611684
KIAA0156	Squamous cell carcinoma antigen recognized by T cells 3	611684
TIP110	Squamous cell carcinoma antigen recognized by T cells 3	611684
SLC10A2	Solute carrier family 10 (sodium/bile acid cotransporter family), member 2	601295
NTCP2	Solute carrier family 10 (sodium/bile acid cotransporter family), member 2	601295
PBAM	Solute carrier family 10 (sodium/bile acid cotransporter family), member 2	601295
SLC10A1	Solute carrier family 10 (sodium/bile acid cotransporter family), member 1	182396
NTCP1	Solute carrier family 10 (sodium/bile acid cotransporter family), member 1	182396
HDMCP	Hepatocellular carcinoma-downregulated mitochondrial carrier protein	609911
C14orf68	Hepatocellular carcinoma-downregulated mitochondrial carrier protein	609911
HCCAT5	Hepatocellular carcinoma-associated transcript 5	615613
HTA	Hepatocellular carcinoma-associated transcript 5	615613
MSPC	Palmoplantar carcinoma, multiple self-healing	616964
ICT1	Immature colon carcinoma transcript 1	603000
DS1	Immature colon carcinoma transcript 1	603000
DCC	Deleted in colorectal carcinoma	120470
MRMV1	Deleted in colorectal carcinoma	120470
HGPPS2	Deleted in colorectal carcinoma	120470
SERPINB4	Serpin peptidase inhibitor, clade B (ovalbumin), member 4 (squamous cell carcinoma antigen 2)	600518
SCCA2	Serpin peptidase inhibitor, clade B (ovalbumin), member 4 (squamous cell carcinoma antigen 2)	600518

Gene/locus	Gene/locus name	Gene/locus MIM number
SERPINB3	Serpin peptidase inhibitor, clade B (ovalbumin), member 3 (squamous cell carcinoma antigen 1)	600517
SCCA1	Serpin peptidase inhibitor, clade B (ovalbumin), member 3 (squamous cell carcinoma antigen 1)	600517
TCO	Thyroid carcinoma, nonmedullary, with cell oxyphilia	603386
BCAS4	Breast carcinoma amplified sequence 4	607471
BCAS1	Breast carcinoma amplified sequence	602968
NABC1	Breast carcinoma amplified sequence	602968
PICRAR	p38-inhibited cutaneous squamous cell carcinoma-associated long intergenic noncoding RNA	617191
LINC00162	p38-inhibited cutaneous squamous cell carcinoma-associated long intergenic noncoding RNA	617191
NLC1C	p38-inhibited cutaneous squamous cell carcinoma-associated long intergenic noncoding RNA	617191
SLC10A3	Solute carrier family 10 (sodium/bile acid cotransporter family) member 3 (protein p3)	312090
P3	Solute carrier family 10 (sodium/bile acid cotransporter family) member 3 (protein p3)	312090

References:

- Khan SA, Taylor-Robinson SD, Toledano MB et al: Changing international trends in mortality rates for liver, biliary and pancreatic tumours. *J Hepatol*, 2002; 37(6): 806–13
- Saha SK, Zhu AX, Fuchs CS, Brooks GA: Forty-year trends in cholangiocarcinoma incidence in the U.S.: Intrahepatic disease on the rise. *Oncologist*, 2016; 21(5): 594–99
- Khan SA, Davidson BR, Goldin RD et al: Guidelines for the diagnosis and treatment of cholangiocarcinoma: An update. *Gut*, 2012; 61(12): 1657–69
- Iwahashi S, Ishibashi H, Utsunomiya T et al: Effect of histone deacetylase inhibitor in combination with 5-fluorouracil on pancreas cancer and cholangiocarcinoma cell lines. *J Med Invest*, 2011; 58(1–2): 106–9
- Valle J, Wasan H, Palmer DH et al: Cisplatin plus gemcitabine versus gemcitabine for biliary tract cancer. *N Engl J Med*, 2010; 362(14): 1273–81
- Fabricant DS, Farnsworth NR: The value of plants used in traditional medicine for drug discovery. *Environ Health Perspect*, 2001; 109(Suppl. 1): 69–75
- Kuttan G, Menon LG, Antony S, Kuttan R: Anticarcinogenic and antimetastatic activity of Iscador. *Anticancer Drugs*, 1997; 8(Suppl. 1): S15–16
- Kwon SB, Kim MJ, Yang JM et al: *Cudrania tricuspidata* stem extract induces apoptosis via the extrinsic pathway in SiHa cervical cancer cells. *PLoS One*, 2016; 11(3): e0150235
- Zarkovic N, Kalisnik T, Loncaric I et al: Comparison of the effects of *Viscum album* lectin ML-1 and fresh plant extract (Isorel) on the cell growth *in vitro* and tumorigenicity of melanoma B16F10. *Cancer Biother Radiopharm*, 1998; 13(2): 121–31
- Yang Z, Zhu S, Liu S et al: Anticancer effect of fufang yiliu yin on human hepatocellular carcinoma SMMC-7721 cells. *Am J Transl Res*, 2018; 10(2): 491–500
- Shao BM, Xu W, Dai H et al: A study on the immune receptors for polysaccharides from the roots of *Astragalus membranaceus*, a Chinese medicinal herb. *Biochem Biophys Res Commun*, 2004; 320(4): 1103–11
- Li S, Wang D, Tian W et al: Characterization and anti-tumor activity of a polysaccharide from *Hedysarum polybotrys* Hand.-Mazz. *Carbohydrate Polymers*, 2008; 73(2): 344–50
- Geng G, Du HX et al: [Experimental study on growth inhibition of Astragalus on lung adenocarcinoma cells.] *Pract Clin J Integr Tradit Chin West Med*, 2011; 2011; 4–5 [in Chinese]
- Song Y, Bai WL: [Effect of astragalus on cell proliferation and apoptosis in laryngeal carcinoma cell line.] *Pract Pharm Clin Remed*, 2013; 16: 5–7 [in Chinese]
- Zhang Z: [Effect of total glucosides of Astragalus on the viability of SCC15 oral cancer cells and its mechanism.] *Chin Pract Med*, 2013; 8: 249–50 [in Chinese]
- Li R, Chen W, Wang W et al: Extraction, characterization of Astragalus polysaccharides and its immune modulating activities in rats with gastric cancer. *Carbohydrate Polymers*, 2009; 78(4): 738–42
- Xu Y BG, Wu MY: [The effect of Huangqi Injection on immune function in rats with scald.] *Chin Tradit Patent Med*, 2000; 22: 494–96 [in Chinese]
- Jin H: Immunomodulatory effects of Astragalus membranaceus and Astragalus polysaccharides from IL-2. *Chin J Immunol*, 1989; 308–10 [in Chinese]
- XianBo WU, QuanYu DU, Liang YL, Ping MA: Effects of Astragalus polysaccharide on immune function of lung-qi deficiency model mice. *China Pharmacy*, 2012; 23(47): 4417–18
- Li R, Ma X, Song Y et al: Anti-colorectal cancer targets of resveratrol and biological molecular mechanism: Analyses of network pharmacology, human and experimental data. *J Cell Biochem*, 2019 [Epub ahead of print]
- Su M, Guo C, Liu M et al: Therapeutic targets of vitamin C on liver injury and associated biological mechanisms: A study of network pharmacology. *Int Immunopharmacol*, 2019; 66: 383–87
- Bi YH, Zhang LH, Chen SJ, Ling QZ: Antitumor mechanisms of curcumae rhizoma based on network pharmacology. *Evid Based Complement Alternat Med*, 2018; 2018: 4509892
- Hu Y, Chen D: Analysis of the action mechanism of Fang Ji Huang Qi decoction in treating rheumatoid arthritis by network pharmacology. *Traditional Medicine Research*, 2018; (6): 286–94
- Alves-Silva JM, Romane A, Efferth T, Salgueiro L: North African medicinal plants traditionally used in cancer therapy. *Front Pharmacol*, 2017; 8: 383
- Shi XQ, Yue SJ, Tang YP et al: A network pharmacology approach to investigate the blood enriching mechanism of Danggui buxue Decoction. *J Ethnopharmacol*, 2019; 235: 227–42
- Ru J, Li P, Wang J et al: TCMSP: A database of systems pharmacology for drug discovery from herbal medicines. *J Cheminform*, 2014; 6: 13

27. Stelzer G, Rosen N, Plaschkes I et al: The GeneCards Suite: From gene data mining to disease genome sequence analyses. *Curr Protoc Bioinformatics*, 2016; 54: 1.30.1–1.30.33
28. Amberger JS, Hamosh A: Searching Online Mendelian Inheritance in Man (OMIM): A knowledgebase of human genes and genetic phenotypes. *Curr Protoc Bioinformatics*, 2017; 58: 1.2.1–1.2.12
29. Oliveros JC: VENNY. An interactive tool for comparing lists with Venn Diagrams. <https://bioinfogp.cnb.csic.es/tools/venny/index.html>
30. Shannon P, Markiel A, Ozier O et al: Cytoscape: A software environment for integrated models of biomolecular interaction networks. *Genome Res*, 2003; 13(11): 2498–504
31. Szklarczyk D, Morris JH, Cook H et al: The STRING database in 2017: quality-controlled protein-protein association networks, made broadly accessible. *Nucleic Acids Res*, 2017; 45(D1): D362–68
32. Yu G, Wang LG, Han Y, He QY: clusterProfiler: An R package for comparing biological themes among gene clusters. *OMICS*, 2012; 16(5): 284–87
33. The Gene Ontology Consortium: Expansion of the Gene Ontology knowledgebase and resources. *Nucleic Acids Res*, 2017; 45(D1): D331–38
34. Kanehisa M, Goto S: KEGG: Kyoto Encyclopedia of Genes and Genomes. *Nucleic Acids Res*, 2000; 28(1): 27–30
35. Kanehisa M, Furumichi M, Tanabe M et al: KEGG: New perspectives on genomes, pathways, diseases and drugs. *Nucleic Acids Res*, 2017; 45(D1): D353–61
36. Li B, Severson E, Pignon JC et al: Comprehensive analyses of tumor immunity: Implications for cancer immunotherapy. *Genome Biol*, 2016; 17(1): 174
37. Li T, Fan J, Wang B et al: TIMER: A web server for comprehensive analysis of tumor-infiltrating immune cells. *Cancer Med*, 2017; 7(21): e108–10
38. Ohtani H: Focus on TILs: Prognostic significance of tumor infiltrating lymphocytes in human colorectal cancer. *Cancer Immun*, 2007; 7: 4
39. Azimi F, Scolyer RA, Rumcheva P et al: Tumor-infiltrating lymphocyte grade is an independent predictor of sentinel lymph node status and survival in patients with cutaneous melanoma. *J Clin Oncol*, 2012; 30(21): 2678–83
40. Yoshihara K, Shahmoradgoli M, Martinez E et al: Inferring tumour purity and stromal and immune cell admixture from expression data. *Nat Commun*, 2013; 4: 2612
41. Hoyos S, Navas MC, Restrepo JC, Botero RC: Current controversies in cholangiocarcinoma. *Biochim Biophys Acta Mol Basis Dis*, 2018; 1864(4 Pt B): 1461–67
42. Zhang GB, Li QY, Chen QL, Su SB: Network pharmacology: A new approach for Chinese herbal medicine research. *Evid Based Complement Alternat Med*, 2013; 2013: 621423
43. Brito AF, Ribeiro M, Abrantes AM et al: New approach for treatment of primary liver tumors: The role of quercetin. *Nutr Cancer*, 2016; 68(2): 250–66
44. Senggunprai L, Kukongviriyapan V, Prawan A, Kukongviriyapan U: Quercetin and EGCG exhibit chemopreventive effects in cholangiocarcinoma cells via suppression of JAK/STAT signaling pathway. *Phytother Res*, 2014; 28(6): 841–48
45. Cui Y, Morgenstern H, Greenland S et al: Dietary flavonoid intake and lung cancer – a population-based case-control study. *Cancer*, 2008; 112(10): 2241–48
46. Bobe G, Weinstein SJ, Albanes D et al: Flavonoid intake and risk of pancreatic cancer in male smokers (Finland). *Cancer Epidemiol Biomarkers Prev*, 2008; 17(3): 553–62
47. Chen AY, Chen YC: A review of the dietary flavonoid, kaempferol on human health and cancer chemoprevention. *Food Chem*, 2013; 138(4): 2099–107
48. Qin Y, Cui W, Yang X, Tong B: Kaempferol inhibits the growth and metastasis of cholangiocarcinoma *in vitro* and *in vivo*. *Acta Biochim Biophys Sin*, 2016; 48(3): 238–45
49. Walters J, Pop C, Scott FL et al: A constitutively active and uninhibitable caspase-3 zymogen efficiently induces apoptosis. *Biochem J*, 2009; 424(3): 335–45
50. Perry DK, Smyth MJ, Stennicke HR et al: Zinc is a potent inhibitor of the apoptotic protease, caspase-3. A novel target for zinc in the inhibition of apoptosis. *J Biol Chem*, 1997; 272(30): 18530–33
51. Roskoski R Jr.: ERK1/2 MAP kinases: Structure, function, and regulation. *Pharmacol Res*, 2012; 66(2): 105–43
52. Nishikawa Y, Sone M, Nagahama Y et al: Tumor necrosis factor-alpha promotes bile ductular transdifferentiation of mature rat hepatocytes *in vitro*. *J Cell Biochem*, 2013; 114(4): 831–43
53. Yuan D, Huang S, Berger E et al: Kupffer cell-derived tnf triggers cholangiocellular tumorigenesis through JNK due to chronic mitochondrial dysfunction and ROS. *Cancer Cell*, 2017; 31(6): 771–89.e776
54. Dang Chi V: MYC on the path to cancer. *Cell*, 2012; 149(1): 22–35
55. Yang H, Li TW, Ko KS et al: Switch from Mnt-Max to Myc-Max induces p53 and cyclin D1 expression and apoptosis during cholestasis in mouse and human hepatocytes. *Hepatology* (Baltimore, Md), 2009; 49(3): 860–70
56. Barr S, Thomson S, Buck E et al: Bypassing cellular EGF receptor dependence through epithelial-to-mesenchymal-like transitions. *Clin Exp Metastasis*, 2008; 25(6): 685–93
57. Sebastian S, Settleman J, Reshkin SJ et al: The complexity of targeting EGFR signalling in cancer: from expression to turnover. *Biochim Biophys Acta*, 2006; 1766(1): 120–39
58. Henson ES, Gibson SB: Surviving cell death through epidermal growth factor (EGF) signal transduction pathways: implications for cancer therapy. *Cell Signal*, 2006; 18(12): 2089–97
59. Yoshikawa D, Ojima H, Iwasaki M et al: Clinicopathological and prognostic significance of EGFR, VEGF, and HER2 expression in cholangiocarcinoma. *Br J Cancer*, 2008; 98(2): 418–25
60. Harder J, Waiz O, Otto F et al: EGFR and HER2 expression in advanced biliary tract cancer. *World J Gastroenterol*, 2009; 15(36): 4511–17
61. Yoon JH, Gwak GY, Lee HS et al: Enhanced epidermal growth factor receptor activation in human cholangiocarcinoma cells. *J Hepatol*, 2004; 41(5): 808–14
62. Ito Y, Takeda T, Sasaki Y et al: Expression and clinical significance of the erbB family in intrahepatic cholangiocellular carcinoma. *Pathol Res Pract*, 2001; 197(2): 95–100
63. Claperon A, Guedj N, Mergely M et al: Loss of EBP50 stimulates EGFR activity to induce EMT phenotypic features in biliary cancer cells. *Oncogene*, 2012; 31(11): 1376–88
64. Nonomura A, Ohta G, Nakanuma Y et al: Simultaneous detection of epidermal growth factor receptor (EGF-R), epidermal growth factor (EGF) and ras p21 in cholangiocarcinoma by an immunocytochemical method. *Liver*, 1988; 8(3): 157–66
65. Claperon A, Mergely M, Nguyen Ho-Bouloires TH et al: EGF/EGFR axis contributes to the progression of cholangiocarcinoma through the induction of an epithelial-mesenchymal transition. *J Hepatol*, 2014; 61(2): 325–32
66. Herceg Z, Wang ZQ: Functions of poly(ADP-ribose) polymerase (PARP) in DNA repair, genomic integrity and cell death. *Mutat Res*, 2001; 477(1–2): 97–110
67. Ratnam K, Low JA: Current development of clinical inhibitors of poly(ADP-ribose) polymerase in oncology. *Clin Cancer Res*, 2007; 13(5): 1383–88
68. Mao Y, Huang X, Shuang Z et al: PARP inhibitor olaparib sensitizes cholangiocarcinoma cells to radiation. *Cancer Med*, 2018; 7(4): 1285–96
69. Galon J, Angell HK, Bedognetti D, Marincola FM: The continuum of cancer immunosurveillance: Prognostic, predictive, and mechanistic signatures. *Immunity*, 2013; 39(1): 11–26
70. Pages F, Mlecnik B, Marliot F et al: International validation of the consensus Immunoscore for the classification of colon cancer: A prognostic and accuracy study. *Lancet*, 2018; 391(10135): 2128–39
71. Angelova M, Mlecnik B, Vasaturo A et al: Evolution of metastases in space and time under immune selection. *Cell*, 2018; 175(3): 751–65.e716
72. Ciardiello F, Tortora G: EGFR antagonists in cancer treatment. *N Engl J Med*, 2008; 358(11): 1160–74
73. Harari PM, Allen GW, Bonner JA: Biology of interactions: anti-epidermal growth factor receptor agents. *J Clin Oncol*, 2007; 25(26): 4057–65
74. Pao W, Miller VA, Politi KA et al: Acquired resistance of lung adenocarcinomas to gefitinib or erlotinib is associated with a second mutation in the EGFR kinase domain. *PLoS Med*, 2005; 2(3): e73